Enhanced Functionality For Donor-Acceptor Oligothiophenes via Inclusion of BODIPY: Synthesis, Electrochemistry, Photophysics and Model Chemistry

Daniel Collado[1], Juan Casado*[2], Sandra Rodríguez González[2], Juan T. López Navarrete*[2], Rafael Suau[1], Ezequiel Perez-Inestrosa*[1], Ted. M. Pappenfus[3], M Manuela M. Raposo[4]

[1]Department of Organic Chemistry, University of Málaga, Campus de Teatinos s/n, Málaga 29071, Spain

[2]Department of Physical Chemistry, University of Málaga, Campus de Teatinos s/n, Málaga 29071, Spain

[3]Division of Science and Mathematics, University of Minnesota Morris, MN 56267, USA

[4]Center of Chemistry, University of Minho, Campus de Gualtar, 4710-057 Braga, Portugal

*To whom correspondence should be addressed. E−mail: (J.C.) casado@uma.es, teodomiro@uma.es

Abstract

We have synthesized several new push-pull oligothiophenes based on the BODIPY moiety as the electron acceptor and the well known oligothiophenes substituted with *N,N*-dialkylamino groups to enhance the electron donor ability. A complete characterization of the electronic properties has been done consisting of their photophysical, electrochemical and vibrational properties. The compounds have been studied after chemical treatment with acids and after oxidation. In this regard, they can be termed as NIR dyes and amphoteric redox electroactive molecules. We have described the presence of dual fluorescence in these molecules and fluorescence quenching either by energy transfer or, in the push-pull molecules, by the electron exchange. The combination of electrochemical and proton reversibility combined with the interesting optical properties of the new species offer an interesting platform for sensor and material applications.

I.   Introduction

Oligothiophenes are often utilized as building blocks in the preparation of organic materials for use as organic semiconductors. This is due in large part because of their excellent electronic properties and other features such as chemical resistance, relative ease of synthesis and proccesability, etc.[1] As a result, there are many classes of oligothiophenes serving in applications such as organic field-effect transistors,[2] organic light-emitting diodes,[3] optically pumped lasers,[4] photovoltaics,[5] non-linear optics,[6] and biology.[7] From a chemical point of view, innovation in this field must pursue the exploration of different ways of molecular conjugation, for instance, with the implementation of new functional groups able to incorporate distinctive and singular properties.

4,4-Difluoro-4-bora-3a,4a-diaza-*s*-indacene (i.e., BODIPY) exhibits excellent photophysical properties (sharp fluorescence emissions and high fluorescence quantum yields) as well as high photo-stability.[8] In addition given its particular structure, amphoteric redox behavior can be exploited since it can act as a donor or an acceptor. All of these features make the BODIPY fragment potentially useful in the field of organic electronics. Despite the many reports of oligothiophenes, only a couple of cases, however, have been reported combining the properties of oligothiophenes and BODIPY containing mono- or di-substitution of the terminal α–position of linear oligothiophenes.[9] This investigation aims to investigate further the coupling of BODIPY with oligothiophenes in donor-acceptor materials.

Intramolecular charge transfer (i.e., ICT) is commonly induced by connecting an electron-donor and a electron-acceptor via a conjugated bridge in such a way that the electron polarization and/or electron transfer, among other factors, are modulated by the polarisable electron structure of the bridge (e.g., nature of the conjugated units and number, bridge conformation, etc.).[10] This ICT

gives rise to a series of properties such as intense visible absorptions, amphoteric redox behavior, and enhanced non-linear optical responses. [6, 10]

In this work, a new series of compounds combining the properties of oligothiophenes and BODIPY in a donor-acceptor chemical architecture are presented. The oligothiophene-to-BODIPY connection goes through the *meso* position of the latter giving rise to a cross-conjugated disposition relative to the linear conjugated sequence in the oligothiophene moiety. Consequently we are investigating the electronic and optical properties promoted by the bonding of oligothiophenes and BODIPY in a donor-to-acceptor configuration (i.e., promoting the appearance of an ICT property) together with the effect of cross-conjugation and their relevance to organic materials.

A detailed spectroscopic, electrochemical, photophysical and theoretical study is described, highlighting the main molecular features of the thienyl-BODIPY combination. As a whole, absorption and emission properties, vibrational spectra and cyclic voltammetry data are comprehensively studied with quantum-chemical calculations. These resulting features will be described: i) structure-function relationships, ii) proton-triggered and selective chemical oxidation reactions and the description of their relevant optical properties together with their visualization in chemical sensing, and iii) *per se* these samples will be viewed as NIR absorbers and dual redox actors with importance of these properties in solar cells design.

II.   Experimental and Theoretical Details.

II. 1. Materials and General Synthesic Procedure.

All reactions were carried out under an argon atmosphere unless otherwise noted. CH_2Cl_2 was distilled from calcium hydride or phosphorus pentoxide. Commercial grade reagents and solvents were used without further purification unless otherwise stated. ^{1}H and ^{13}C-NMR spectra were recorded on a Bruker instrument at 200 MHz (^{1}H) and 52 MHz (^{13}C). NMR chemical shift are

expressed in parts per millon relative to internal solvent peak, and coupling constants were measured in Hertz. Products were purified by silica gel chromatography (SiO$_2$ 15-40 μm). The synthesis of non commercial 5'-formyl-5-*N,N*-dimelthylamino-2,2'-bithiophene and 5''-Formyl-5-*N,N*-dimethylamino-2,2':5'2''-terthiophene were previously described.[11]

General synthesis of BODIPY oligothiophenes. 2,2'-Bithiophene-5-carboxaldehyde (200 mg, 1 mmol) was dissolved in neat pyrrole (1 mL, 14.4 mmol), and 3 drops of trifluoroacetic acid (TFA) were added. The reaction was allowed to proceed for 2.5 h at room temperature and directly oxidized with a solution of DDQ (227 mg, 1 mmol) in CH$_2$Cl$_2$ (10 mL) at room temperature. The reaction was allowed to proceed for 4 h at room temperature. Triethylamine (1.73 mL, 12.39 mmol) was added to the solution, which was stirred for 30 min. BF$_3$:Et$_2$O (2.11 mL, 16.64 mmol) was added, and stirring was maintained for 1 h. The reaction mixture was washed with H$_2$O (2x50ml) and the aqueous solution was extracted with CH$_2$Cl$_2$. The combined organic layers were dried over anh. MgSO$_4$, filtered, and evaporated. The crude product was purified by silica gel column chromatography (CH$_2$Cl$_2$:ciclohexane; 1:1) to afford BODIPY compound. Further purification was undertaken by preparative TLC.

5-Bodipy-2,2'-bithiophene (BPY-2T). Red powder, (148 mg, 41%) mp 124-126 ºC. R$_F$ = 0.3 CH$_2$Cl$_2$:cyclohexane; 1:2. ^{1}H NMR (CDCl$_3$, 200 MHz) δ (ppm) 7.91 (s, 2H), 7.50 (d, 1H , *J* = 3.8 Hz), 7.35-7.31 (m , 5H), 7.08 (dd, 1H, *J* = 5.4, 4.8 Hz), 6.58 (m, 2H) ; ^{13}C NMR (CDCl$_3$, 52 MHz) δ (ppm) 144.2, 143.4, 135.7, 134.3, 133.9, 132.9, 131.0, 128.3, 126.5, 125.4 ,124.7, 118.4, 118.3; HRMS *m/z*: Calcd for C$_{17}$H$_{11}$BF$_2$N$_2$NaS$_2$: 379.0317. Found: 379.0329; UV-vis (CH$_2$Cl$_2$) λ_{max} (ε): 514 (33,170), 312 (8,232).

5-Bodipy-5'-*N,N*-diisopropylamino-2,2'-bithiophene (BPY-2T-N(i-Pr)$_2$). Purple powder, (56 mg, 45%). mp decomposes > 150 ºC. ^{1}H NMR (CDCl$_3$, 200 MHz) δ (ppm) 7.84 (s, 2H), 7.54 (d, 1H, *J* = 3.8 Hz), 7.36 (d, 2H, *J* = 4.3 Hz), 7.11 (d, 1H, *J* = 4.3 Hz), 7.08 (d, 1H, *J* = 4.3 Hz), 6.55-6.54 (m, 2H), 6.4 (d, 1H, *J* = 3.8 Hz), 3.77 (septuplet, 2H, *J* = 7.0 Hz), 1.30 (d, 12H, *J* = 7.0 Hz);

^{13}C NMR (CDCl$_3$, 52 MHz) δ (ppm) 157.5, 157.0, 147.9, 136.1, 129.9, 126.4, 126.5, 121.6, 121.7, 117.5, 117.5, 117.6, 107.4, 51.3, 20.4; HRMS *m/z*: Calcd for C$_{23}$H$_{24}$BF$_2$N$_3$S$_2$: 455.1467. Found: 455.1477 ; UV-vis (CH$_2$Cl$_2$) λ_{max} (ε): 708 (22,271), 510 (35,815), 380 (14,156).

5-Bodipy-5''-*N,N*-dimethylamino-2,2':5'2''-terthiophene (BPY-3T-N(Me)$_2$). Purple powder, (55 mg, 43%). mp decomposes > 170ºC. ^{1}H NMR (CDCl$_3$, 200 MHz) δ (ppm) 7.89 (s, 2H), 7.51 (d, 1H, *J* = 3.8 Hz), 7.35 (d, 2H, *J* = 4.3 Hz), 7.25 (m, 1H), 7.19 (d, 1H, *J* = 3.8 Hz), 6.95 (d, 1H, *J* = 3.8 Hz), 6.87 (d, 1H, *J* = 3.8 Hz), 6.57 (m, 2H), 5.79 (d, 1H, *J* = 4.3 Hz), 2.96 (s, 6H); ^{13}C NMR (CDCl$_3$, 52 MHz) δ (ppm) 159.5, 145.1, 142.9, 140.6, 134.9, 132.2, 133.7, 130.6, 126.4, 125.0, 123.9, 121.4, 120.3, 118.1, 120.3, 102.6, 42.5, 29.6; HRMS *m/z*: Calcd for C$_{23}$H$_{18}$BF$_2$N$_3$S$_3$: 481.0718. Found: 481.0719 ; UV-vis (CH$_2$Cl$_2$) λ_{max} (ε): 628 (14,156), 514 (36,210), 406 (8,652).

II. 2. Spectroscopic measurements. UV-Vis absorption spectra were recorded on an Agilent 8453 instrument equipped with a diode array detection system. Emission spectra were measured using a spectrofluorimeter from Edinburgh Analytical Instrument (FLS920P) equipped with a pulsed xenon flash-lamp. Fluorescence quantum yields, ϕ_F, were measured for all the solutions using quinine sulphate in 0.1 M H$_2$SO$_4$ (ϕ_F=0.546) as the standard.[12]

1064 nm FT–Raman spectra were measured using an FT–Raman accessory kit (FRA/106–S) of a Bruker Equinox 55 FT–IR interferometer. A continuous–wave Nd–YAG laser working at 1064 nm was used for excitation along with a germanium detector operating at liquid nitrogen temperature. Raman scattering radiation was collected in a back–scattering configuration with a standard spectral resolutions of 4 and 1 cm^{-1}. 1000-3000 scans were averaged for each spectrum. Raman spectra with λ_{exc} = 532 nm were recorded by using a Senterra dispersive Raman microscope from Bruker. UV-Vis-NIR and Raman spectro-chemistry were done by protonation with trifluoroacetic acid and chemical oxidation using FeCl$_3$ as the oxidant in dried dichloromethane.

II. 3. Electrochemical Measurements.   Room temperature electrochemical measurements were performed with a BAS 100B electrochemical analyzer and C3 cell stand in a three-electrode configuration with a glassy carbon working electrode (A = 0.07 cm^2), a platinum counter electrode, and a standard Ag|AgCl|KCl (1.0 M) reference electrode. A single compartment, low volume cell was used for all measurements. Tetrabutylammonium hexafluorphosphate electrolyte solution was added to the cell (5 mL, 0.1 M/CH$_2$Cl$_2$) and background cyclic voltammograms of the electrolyte solution were recorded prior to the addition of the sample. Suitable amounts of sample were added to create 0.5 mM solutions. The E^0 values for the ferrocenium/ferrocene couple for concentrations similar to those used in this study were 0.43 V for dichloromethane solutions at a glassy carbon electrode. Anodic-cathodic peak separations were typically 80-90 mV for this redox couple.

II. 4. Theoretical Calculations. Density functional theory has a good track record as far as predicting the electronic structure of neutral and charged oligothiophene molecules.[13] DFT has been used for the ground-state properties (i.e., optimized geometries, vibrational spectra, etc.) and time-dependent DFT, or TD-DFT, for the estimation of vertical-adiabatic excited-states transition (i.e., energies and oscillator strengths).[14] The geometries of the relevant excited states were optimized by taking advantage of the restricted single excited configuration interaction approach (CIS) within the Hartree-Fock (HF) approximation, or RCIS/HF, meaning that the single-determinant RHF wavefunction represents the reference determinant in a CIS calculation of excited states.[15]

Most of the calculations were performed with the Gaussian03 suite of programs.[16] For the DFT calculations, Becke's three-parameter (B3) gradient-corrected exchange functional combined with the Lee-Yang-Parr (LYP) correlation functional was used as implemented in Gaussian03.[17] The 6-31G** basis set was taken in the DFT and RCIS/HF calculations.[18] No constraints were imposed during the geometry optimizations. In the TD–DFT calculations, an evaluation of at least the ten lowest-energy vertical electronic excited states was carried out. TD–DFT calculations were performed using the same functional.

III. Results and Discussion

III. 1. Synthesis of BODIPY-nT derivatives. Several formyl-oligothiophenes were used as precursors in the synthesis of BPY-nT derivatives. The synthesis of 5'-formyl-5-*N,N*-dimelthylamino-2,2'-bithiophene and 5''-formyl-5-*N,N*-dimethyl-2,2':5'2''-terthiophene were previously described by some of us by means of metalation followed by reaction with DMF, or through the Stille cross coupling reaction.[11] BPY-nT derivatives have been synthesized starting from the corresponding oligothiophene carbaldehydes in an one-pot, three-step procedure.

Scheme 1. Synthesis of BODIPY compounds.
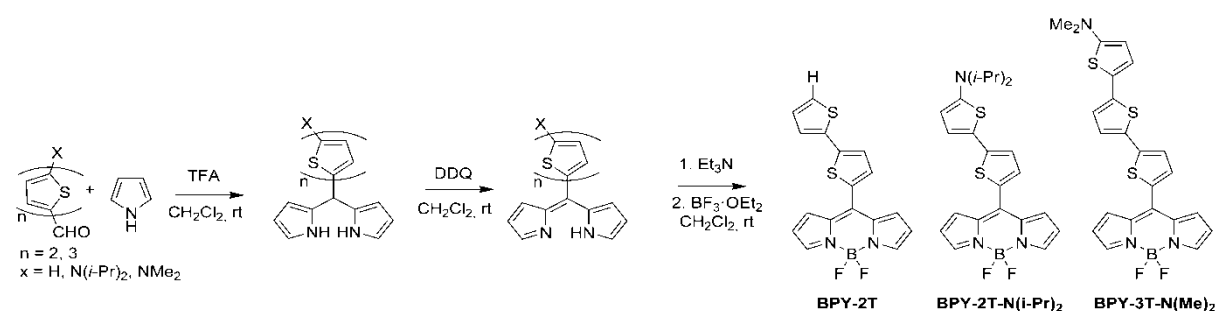
This procedure, according to the usual precedents in the synthesis of BODIPY dyes,[19] is as follows: aldehydes are reacted with a large excess of pyrrole and subsequently, directly oxidized with DDQ, followed by addition of NEt$_3$ and BF$_3$·OEt$_2$. After purification through column chromatography on silica gel the dyads were obtained in 35-40% yields.

III. 2. Absorption Spectra. Figure 2 shows the UV-Vis absorption spectra of the compounds while Table 1 summarizes the main data. To follow the experimental trends, Figure 3 displays the energies of the frontier orbitals (topologies are shown in Figure 4). The covalent union of **2T** and BODIPY (i.e., **BPY**) through the α−terminal at the *meso* positions minimally modifies the spectrum of the bithiophene chromophore revealing the partial decoupling between these two units, an effect possibly ascribed to cross-conjugation interference in the ground electronic state. The band at 314 nm in **2T** corresponds to a one-electron HOMO→LUMO promotion while that a 310 nm in **BPY-2T** is described as a one-electron HOMO−1→LUMO+1 promotion (S$_0$→S$_2$) involving exclusively

the bithienyl unit (i.e., correlated with the HOMO→LUMO excitation in **2T**). Similarly, the band of the BODIPY fragment in **BPY-2T** appears at 514 nm, nearly the same wavelength as free BODIPY at 512 nm, and described as a one-electron HOMO→LUMO transition (S_0→S_1).

Table 1. Absorption[a], emission[b] and electrochemical[c] data for the oligomers.

Oligomer	$\lambda_{max, abs}$ (nm)	$\lambda_{max, em}$ (nm)	ϕ_{fluo}	E^o_{ox} (V)	E^o_{red} (V)
2T	314	362	0.03	$\approx 1.4^d$	-[e]
BODIPY	522	537	0.7	0.96	-1.37
BPY-2T	310, 514	341, 567	0.08, 0.011	1.56^d	-0.70, -1.53^e
BPY-2T-N(i-Pr)$_2$	380, 510, 708	568	0.007	0.54, 1.34^d, 1.70^d	-0.75, -1.59^e
BPY-3T-N(Me)$_2$	406, 514, 614	539	0.006	0.44, 1.03, 1.61^d	-0.71, -1.51^e

[a] In CH_2Cl_2. [b] In CH_2Cl_2. [c] Potentials vs. Ag/AgCl in 0.1 M TBAPF$_6$/CH_2Cl_2 solution. [d] Irreversible process; E_{pa} value provided. [e] Irreversible process; E_{pc} value provided. [f] No observable reduction under the experimental conditions.
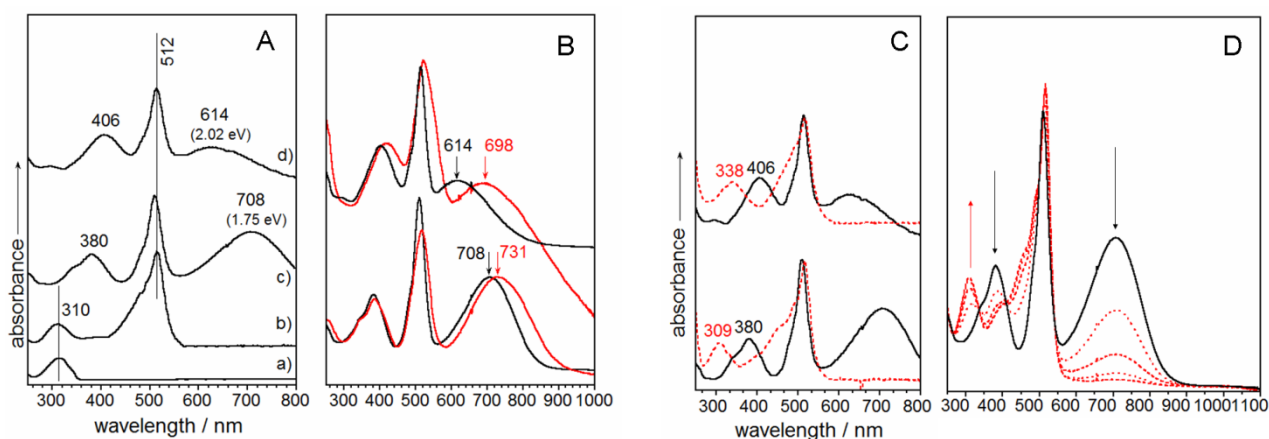

Figure 2. A: UV-Vis electronic absorption spectra in dichloromethane of a) **2T**, b) **BPY-2T**, c) **BPY-2T-N(i-Pr)$_2$**, and **BPY-3T-N(Me)$_2$**. B: Spectra in solution (black lines) and in solid state (red lines) of **BPY-2T-N(i-Pr)$_2$** (bottom) and **BPY-3T-N(Me)$_2$** (up). C: (bottom) spectra of **BPY-2T-N(i-Pr)$_2$** (black) and protonated **BPY-2T-N(i-Pr)$_2$** (red); (top) the spectra of **BPY-3T-N(Me)$_2$** (black) and protonated **BPY-2T-N(i-Pr?)$_2$** (red). D: Titration of **BPY-2T-N(Me)$_2$** with trifluoroacetic acid in dichloromethane.

The attachment of a diisopropyl-amino group at the remaining free bithienyl α–position results in three new features in the absorption spectrum of **BPY-2T-N(i-Pr)$_2$**: i) The bithiophene band is red-shifted by 70 nm indicating the coupling between the two units activated by the inclusion of the lone electron pair of the nitrogen atom; ii) However, the sharp and strong BODIPY band around 510 nm is minimally affected; and iii) The appearance of a new very broad charge transfer band centered at 708 nm. Incorporation of the *N,N*-dialkylamino group improves conjugation with **2T** as evidenced by the HOMO orbital of **BPY-2T-N(i-Pr)$_2$**. This increases its

energy and transforms the BODIPY centered HOMO in **BPY-2T** in a thienyl based orbital in **BPY-2T-N(*i*-Pr)₂**. Consequently, the lowest energy transition, or HOMO→LUMO excitation (S₀→S₁), corresponds now to a **2T-N(*i*-Pr)₂→BODIPY** donor-to-acceptor electron promotion describing an intramolecular charge transfer.
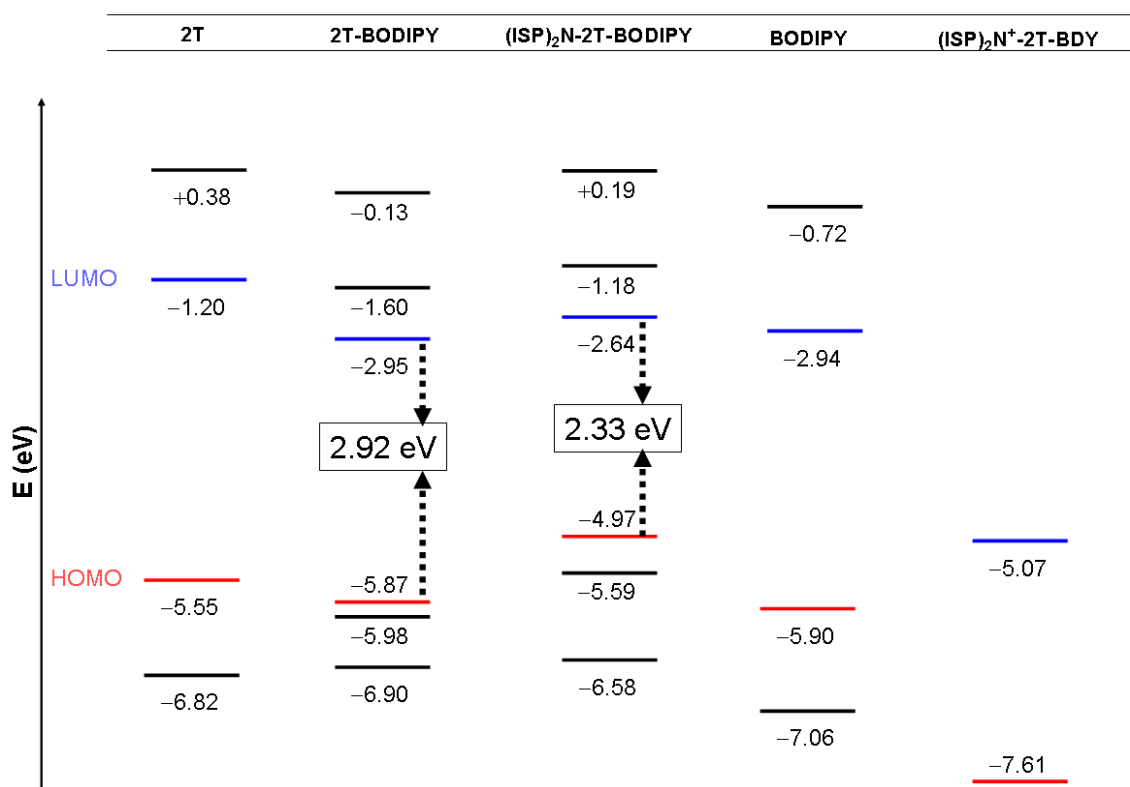

Figure 3. DFT/B3LYP/6-31G** gap orbital energy evolution in the compounds investigated.
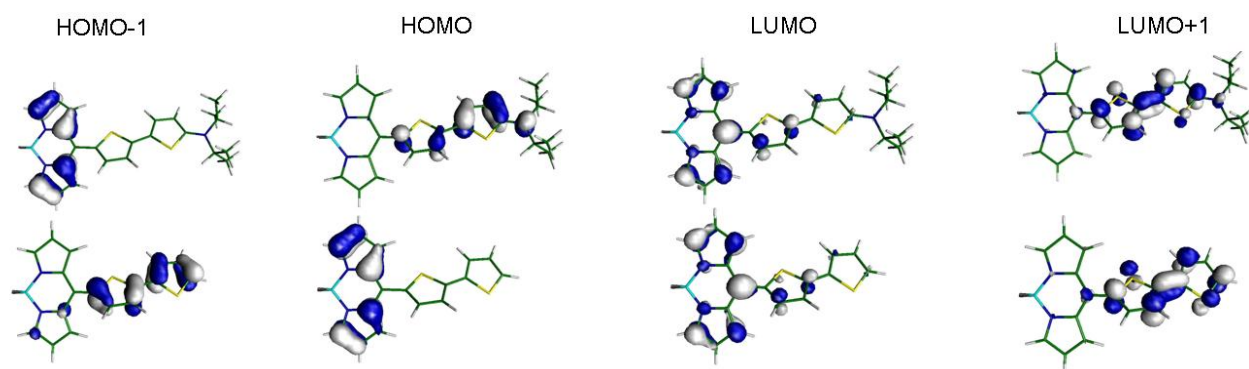

Figure 4. DFT/B3LYP/6-31G** topologies of the relevant orbitals around the gap for **BPY-2T** (bottom) and **BPY-2T-N(*i*-Pr)₂** (top) .

9

Following with this discussion, the elongation of the thienyl chain brings another unexpected result in **BPY-3T-N(Me)$_2$** whose ICT band, measured at the maxima, is blue-shifted relative to the homologous HOMO→LUMO band in **BPY-2T-N(i-Pr)$_2$**. Usually the lengthening of the bridge in linearly connected or linearly conjugated donor-acceptor dyes produced a red-shift of the charge transfer absorption band.[20] Also in Figure 2 the spectra of the two compounds in thin solid films are displayed where a common red-shift of the bands in the solid relative to the solution is observed. This displacement, however, is much more noticeable in **BPY-3T-N(Me)$_2$** resulting that the peak maxima in both compounds are much more similar for the solid state (i.e., 731 nm -1.70 eV- in **BPY-2T-N(i-Pr)$_2$** and 698 nm -1.78 eV- in **BPY-3T-N(Me)$_2$**). This would be interpreted as the intervention of conformers, different to the planar one, in the description of the ground electronic state of **BPY-3T-N(Me)$_2$**). Furthermore the band edges of the charge transfer bands in solid state related with the true optical energy gap are almost coincident in their low energy side likely indicating the saturation of donor-acceptor interaction at the level of the terthiophene bridge. The electrochemical band gap for these two oligomers displays the expected trend, however ?(vide infra).

The presence of the lone electron pair of the amino nitrogen provides another entry for this electronic study given its basicity and potential protonation with a strong acid. In Figures 2C and 2D the absorption spectra of the compounds treated with acid are displayed. It is observed that protonation of the basic center causes the full disappearance of the ICT band and the blue-shift of the thienyl band (from 380 nm to 309 nm) while the BODIPY absorption still remains unaltered. This process is fully reversible (i.e. the CT bands can be fully regenerated) by the addition of a base such as triethylamine. These data demonstrates the fine balance of the gap properties in these BODIPY oligothiophenes which is drastically tuned by inclusion of the appropriate amino group or its chemical protonation. As a result, based on the reversibility of the protonationreaction , interesting spectro-chemical sensor properties can be derived. The HOMO orbital of protonated

BPY-2T-N(*i*-Pr)$_2$ clearly indicates that by removing the conjugatednitrogen lone electron-pair, the donor-to-acceptor connection is switched off.

III. 3. Electrochemical Data. Figure 5 shows the cyclic voltammograms of the compounds in dichloromethane and Table 1 also summarizes the redox potentials. The most relevant feature is the existence of amphoteric redox behavior in **BPY-2T-N(*i*-Pr)$_2$** and **BPY-3T-N(Me)$_2$** which display both reversible reduction and oxidation processes. Oligothiophenes are characterized by their relatively low oxidation potentials resulting in their electron donor properties, a key requirement exploited in their applications as hole transporting materials. In **BPY-2T**, there is an irreversible oxidation at 1.56 V which gives rise to a subsequent typical σ−dimerization process (i.e., revealed by the small peaks in the associated reduction wave).
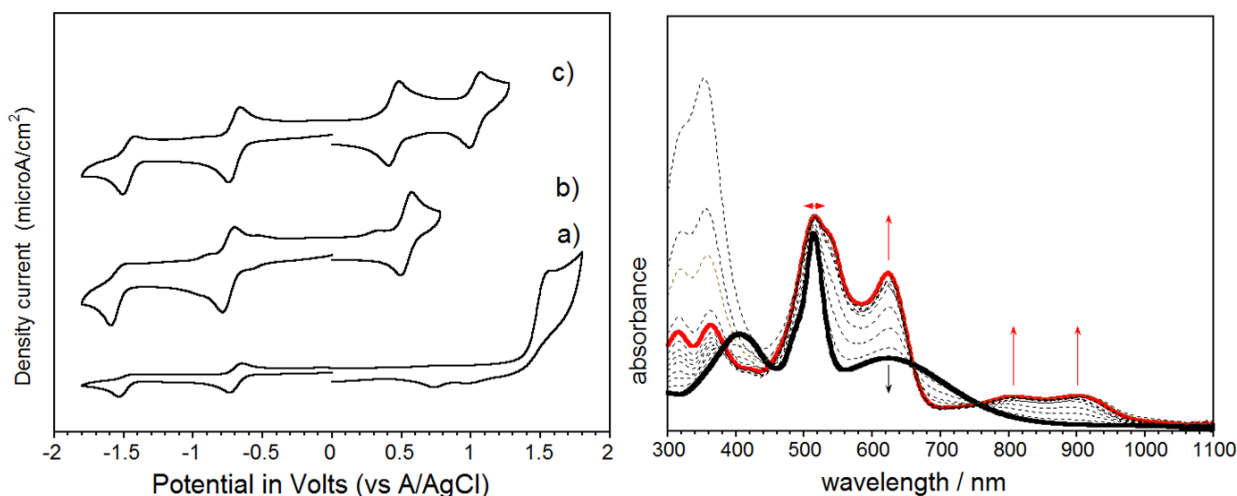

Figure 5. Left: Cyclic voltammetries of a) **BPY-2T**, b) **BPY-2T-N(*i*-Pr)$_2$**, and c) **BPY-3T-N(Me)$_2$** in 0.1 M TBAPF$_6$/CH$_2$Cl$_2$ solutions. Right: UV-Vis-NIR spectrochemistry of **BPY-3T-N(Me)$_2$** in CH$_2$Cl$_2$ by stepwise addition of FeCl$_3$,

The inclusion of the amino functionality in **BPY-2T-N(*i*-Pr)$_2$** results in a dramatic decrease of the first oxidation potential to +0.54 V in agreement with the HOMO orbital to be placed at the extensively conjugated amino-bithienyl fragment [i.e., the HOMO energy goes from −5.87 eV in **BPY-2T** to −4.97 eV in **BPY-2T-N(*i*-Pr)$_2$**]. Increasing the chain length from the dimer to the trimer causes a −0.10 V decrease of the first oxidation processes and a simultaneous stabilization of

the dication at 1.03 V(But in that case the amino group on the trimer is not the same: NMe_2). The first one electron reduction, according to the Koopman´s theorem,[21] occupies the empty LUMOs which, in all the cases, are mainly located at the BODIPY unit (revealing its electron acceptor character) with a slight participation of the directly connected thiophene which will account for the slight variation of the first reduction potentials with the oligothienyl chain. A second reduction appears around −1.5 V being fully reversible only in **BPY-3T-N(Me)$_2$**.

It is relevant to mention the lowest measured electrochemical band gap, 1.15 V (simply calculated by taking the difference between E^0_{ox} and E^0_{red}), in **BPY-3T-N(Me)$_2$** and its homologue optical band gap, around 1.50 eV at the band edge. It is unusual to find the electrochemical band gap lower than the optical band gap which indicates the interesting balance between the donor-to-acceptor interaction. These gap values are in the desired limits of applicability in a series of organic devices, namely, photovoltaics applications. In this regard, these samples can be termed as NIR dyes (i.e., note that NIR dyes are noted for absorption larger than 700 nm) and amphoteric redox electroactive molecules.

Given the interesting electrochemical properties, chemical oxidation of **BPY-3T-N(Me)$_2$** has been performed and monitored by UV-Vis-NIR spectroscopy as represented in Figure 5. Oxidation with one equivalent of $FeCl_3$ gives rise to the spectrum of the radical cation species which has two new intra-gap absorptions around 800 and 900 nm respectively similar to previously characterized terthiophene cation radicals. However the BODIPY absorption at 512 nm keeps its shape and is not altered significantly during the oxidation process while the ICT band at 623 nm is replaced by a new band, sharper and more intense at the same wavelength. Consequently, while protonation induces the disappearance of the ICT band giving rise to a transparent compound in this region, oxidation produces the sample to be a good light absorber in the Vis-NIR region.

III. 4. Photophysical properties. Figure 6 displays the absorption-excitation-fluorescence spectra for **BPY-2T** and **BPY-2T-N(*i*-Pr)₂** while in Table 1 quantum yields are also summarized. Several general features can be extracted from the spectra: i) In all the cases very low fluorescence quantum yields are measured; ii) Dual emission is recorded for the derivatives: one emission comes after excitation the BODIPY band that always yields the typical BODIPY emissions around 560 nm, and the second emission arises either by exciting the thienyl band around 400 nm in **BPY-2T** (i.e., where the typical oligothiophene emission is observed) or for the amine derivatives in which by exciting the same thienyl bands a well red-shifted emission at 510-520 nm is recorded; iv) No emissions are observed by photon pumping the ICT bands at low energy in the push-pull molecules.
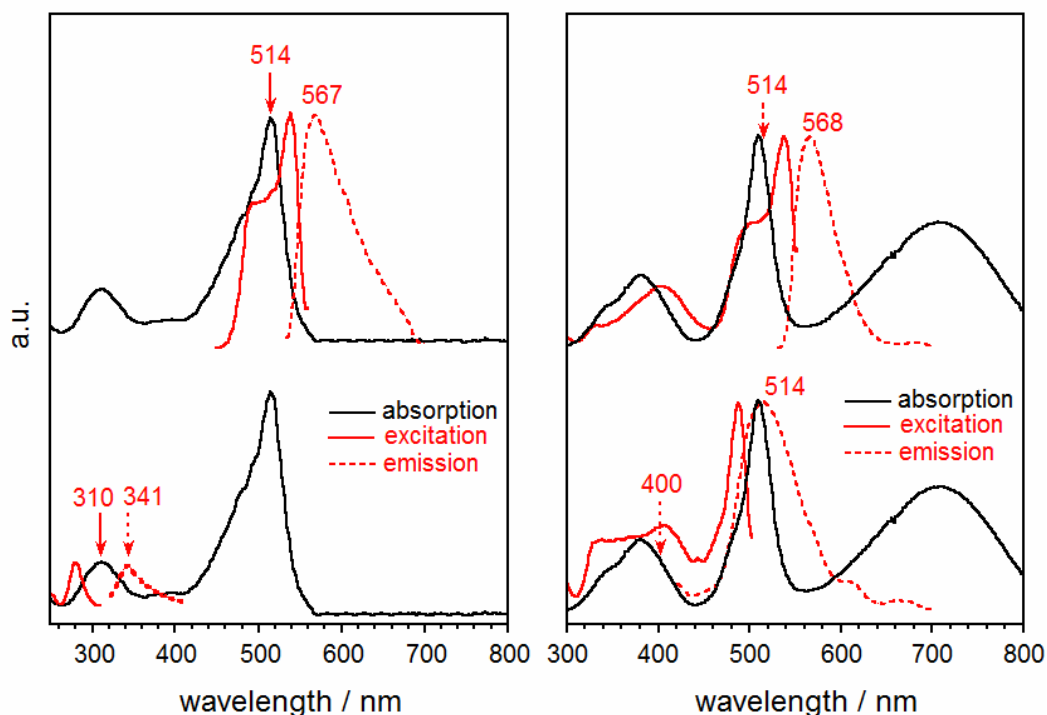

Figure 6. Absorption, excitation and emission spectra of **BPY-2T** (left) and **BPY-2T-N(*i*-Pr)₂** (right) in CH₂Cl₂ solutions.

Overall this means that the covalent bonding of BODIPY and the bithiophene yields a very important minimization of the fluorescence quantum yields compared with the BODIPY group well known to be an excellent emitter, and also allows to the appearance of dual weak fluorescence. In

what follows we will explain these effects assisted with theoretical calculations and electrochemistry.

TD-DFT/B3LYP/6-31G** excited state calculations have been carried out for **BPY-2T** and **BPY-2T-N(i-Pr)$_2$** as the two representative examples to understand the photophysical phenomena. In **BPY-2T** the $S_0 \rightarrow S_1$ excitation is predicted at 463 nm (oscillator strength, f=0.41) and is related with the experimental absorption at 514 nm (extinction coefficient, ε=33,170) that corresponds to a one-electron HOMO$\rightarrow$LUMO transition involving the BODIPY group. The second theoretical band calculated at 310 nm (*f*=0.16) is assigned to the experimental absorption at 310 nm (ε=8,232) and corresponds to a HOMO-1$\rightarrow$LUMO+1 one-electron promotion involving almost exclusively the bithiophene moiety (see Figure 7).
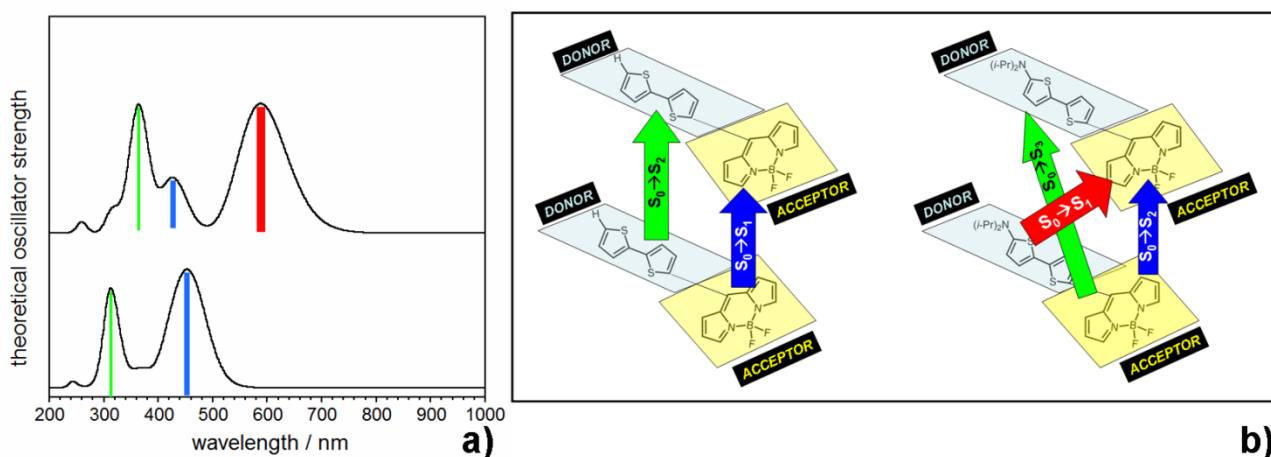

Figure 7. a) TD-DFT/B3LYP/6-31G** theoretical absorption of **BPY-2T** (bottom) and **BPY-2T-N(i-Pr)$_2$** (top); b) Visualization of the inter-chromophore excitation mixing, or ICT transitions, by inclusion of the amino group from **BPY-2T** (left) to **BPY-2T-N(i-Pr)$_2$** (right) according to the TD-DFT/B3LYP/6-31G** theoretical spectra.

In Figure 8 the optimized geometries of the low lying excited states of **BPY-2T** are shown and display nearly identical dihedral angles of ≈ 50 degrees between the BODIPY and thienyl moieties either in S_0 or S_1 indicating how the two units behave independently as for the low energy excited states is concerned. This scenario might produce two different situations: i) the partial decoupling between the two units which can justify the appearance of two different emissions in **BPY-2T** depending on the excitation energy (the situation is also similar to a twisted intramolecular charge transfer –TICT- state with dual emission)[22]; ii) And on the other hand, the quasi-quantitative

quenching of fluorescence detected in **BPY-2T** is an effect already observed in other thiophene-BODIPY dyes and attributed to inter-unit energy transfer by a Förster mechanism.[23] In this regard, the partial spectral overlap between the bithiophene emission and the absorption spectrum of BODIPY will favor the energy transfer process (this process is very efficient in a **BPY-4T** where the spectral overlap of the 4T emission and the BODIPY absorption is much larger than in our **BPY-2T** case).[9]
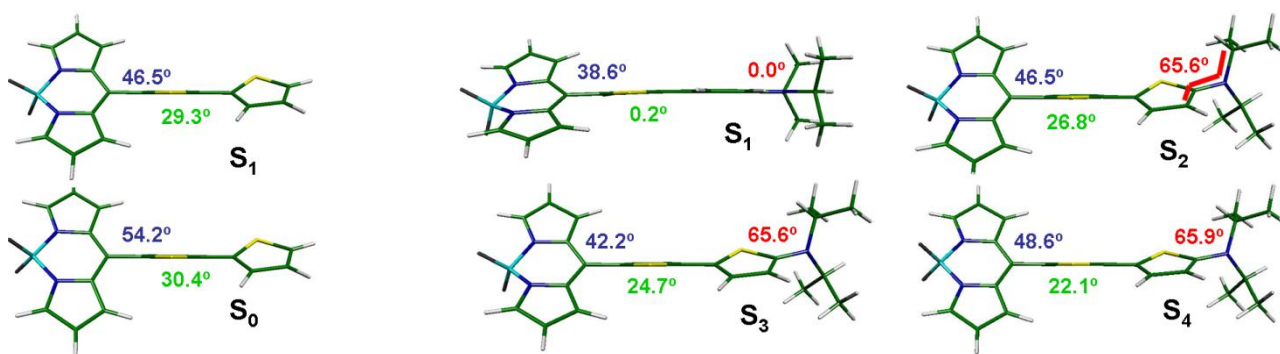

Figure 8. RCIS/HF/6-31G** optimized geometries of the low lying electronic states of **BPY-2T** (left) and **BPY-2T-N(*i*-Pr)$_2$** (right).

For **BPY-2T-N(*i*-Pr)$_2$** the low lying energy excitation $S_0 \rightarrow S_1$ is calculated at 588 nm (*f*=0.58) and appears at 708 nm (ε=22,271) in the absorption spectrum and is composed of a one-electron HOMO$\rightarrow$LUMO transition. In contrast to **BPY-2T** now the HOMO of **BPY-2T-N(*i*-Pr)$_2$** is located at the bithiophene and the LUMO is placed at the BODIPY moiety meaning that the $S_0 \rightarrow S_1$ excitation is an intramolecular donor-to-acceptor charge transfer. As a result of the ICT, and relative to **BPY-2T**, the molecular structure of the lowest energy excited state of **BPY-2T-N(*i*-Pr)$_2$** is significantly co-planarized as shown in Figure 8. The dihedral angle between the BODIPY and thienyl moieties is around almost 38.6º and the angle between the *N,N*-diisopropylamino group and the bithiophene is 0º with the two thiophenes co-planar. Exciting the lowest energy $S_0 \rightarrow S_1$ ICT intramolecular charge transfer, no emission is detected because of the planar and non-radiative character of the intramolecular charge transfer state.

The second excitation, $S_0 \rightarrow S_2$, in **BPY-2T-N(*i*-Pr)$_2$** corresponds to a HOMO-1 to LUMO transition predicted at 426 nm which is related with the 510 nm band in the UV-Vis spectrum.

Given that the HOMO-1 is concentrated in the BODIPY, it turns out that this transition almost exclusively excites the BODIPY unit (see Figure 7) resulting in the typical BODIPY emission at 568 nm. For the $S_1/S_2/S_3$ triad, the largest BODIPY to bithiophene dihedral angle is found for the S_2 (i.e., 46.5º) which reinforces the fact that the excitation/emission process takes place in the BODIPY without affecting other parts of the molecule.
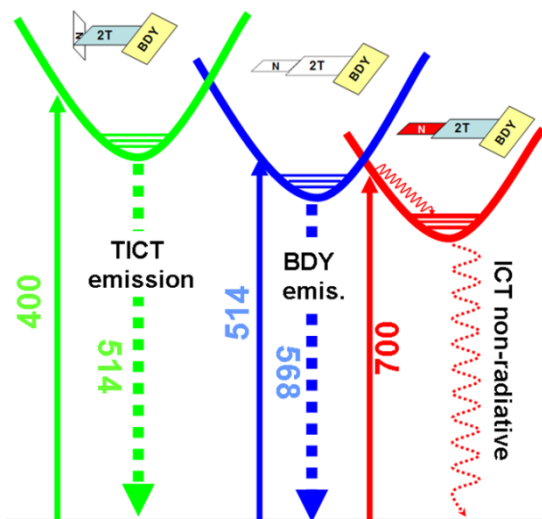

Figure 9. Photophysical scheme proposed for the fluorescence mechanisms of **BPY-2T-N(i-Pr)₂**.

Interestingly, excitation on the bithiophene moiety produces a band at 514 nm, which is a new feature not present in **BPY-2T**. The $S_0 \rightarrow S_3$ excitation in **BPY-2T-N(i-Pr)₂** corresponds to a HOMO-1 to LUMO+1 excitation predicted at 364 nm and observed at 380 nm in its absorption spectrum. Considering that the LUMO+1 orbital is located at the amino-bithiophene unit, it can be described as an acceptor-to-donor excitation, where the driving force has a opposite sense compared to the case of the ICT band at lower energies, that is, a "inverted" charge transfer band (i.e., the electron excitation goes from the acceptor to the donor). As deduced by the optimized geometries of the S_3 (and other excited states close in energy) the bithiophene gets slightly more planar (i.e., 24.7º and 22.1º in S_3 and S_4 respectively) and the angle with the amino group is always large (i.e., $\approx$ 65º) indicating that the electron accumulation in this unit quinoidizes the thienyl backbone and distorts the amino group from the thienyl plane. As a result the p_z nitrogen orbital, with the lone electron

pair, is decoupled from the π−conjugated segment (see that in S_1 the N lone pair is fully conjugated with the bithiophene). This theoretical description would be in line with the appearance of a TICT state (twisted intramolecular charge transfer state) where the twisted feature is found in the amino-donor group, an effect triggered off by the inverse acceptor (BODIPY)→donor (bithiophene) excitation. It is well known the propensity of TICT states to dual emission.

Consequently, the scenario is that two ICT events are observed such as described in Figure 9: a twisted emissive ICT and a planar non-radiative ICT together with an exclusive BODIPY emission. Contrary to **BPY-2T**, in **BPY-2T-N(*i*-Pr)₂** and **BPY-3T-N(Me)₂** the most probable situation to account for the fluorescence quenching is electron exchange, by Dexter mechanism, driven by the improved electron donor properties of the amino-bithiophene moiety relative to the good electron acceptor BODIPY as seen in electrochemical Section III.2 and is related to the small electrochemical gap.[23]

III. 5. Vibrational Raman properties. Figure 10 displays the Raman spectra of the materials. The Raman spectra of the neutral molecules show two groups of bands corresponding to the BODIPY and thiophene moieties at 1550-1530 cm^{-1} and 1450-1430 cm^{-1} respectively. The main Raman band in **BPY-2T** is at 1447 cm^{-1} which is very similar to unsubstituted bithiophene (1442 cm^{-1}). This data indicates that the inclusion of the BODIPY moiety does not significantly modify the π−electron molecular structure of the ground electronic state and is in agreement with the minimal interaction between the two units due to cross-conjugation.

The inclusion of the *N,N*-dialkylamino group in **BPY-2T-N(*i*-Pr)₂** splits the bithiophene band into two components at higher (i.e., 1449 cm^{-1}) and lower (i.e., 1433 cm^{-1}) frequencies relative to **BPY-2T**.[25] This finding reveals the electron donor effect of the amino group on the NR₂-substituted thiophene ring that now vibrates a higher frequency (i.e., 1449 cm^{-1}) as a consequence of the reinforcement of the π−conjugated system. On the other hand, the subtle electron withdrawal effect

of the BODIPY group (i.e., see its role in the ICT electron excitation) causes its closest thiophene rings to be slightly quinoidized resulting in lower ν(C=C) frequency values (i.e., 1433 cm^{-1}). The same phenomena can be described in **BPY-3T-N(Me)$_2$** with two well resolved bands at 1452 cm^{-1} and 1431 cm^{-1} : the former more "aromatic" due to the increasing of the π−conjugational path and the latter slightly more quinoidized arising from the ring connected to the blocking *meso* position of the BODIPY group. As for the BODIPY band, the interaction with the thiophene groups is increasing in the order **BPY-2T** < **BPY-2T-N(*i*-Pr)$_2$** < **BPY-3T-N(Me)$_2$** as denoted by the behavior of the most intense and representative Raman bands at 1548 cm^{-1} in **BPY-2T** at 1543 cm^{-1} in **BPY-2T-N(i-Pr)$_2$** and at 1529 cm^{-1} in **BPY-3T-N(Me)$_2$** .
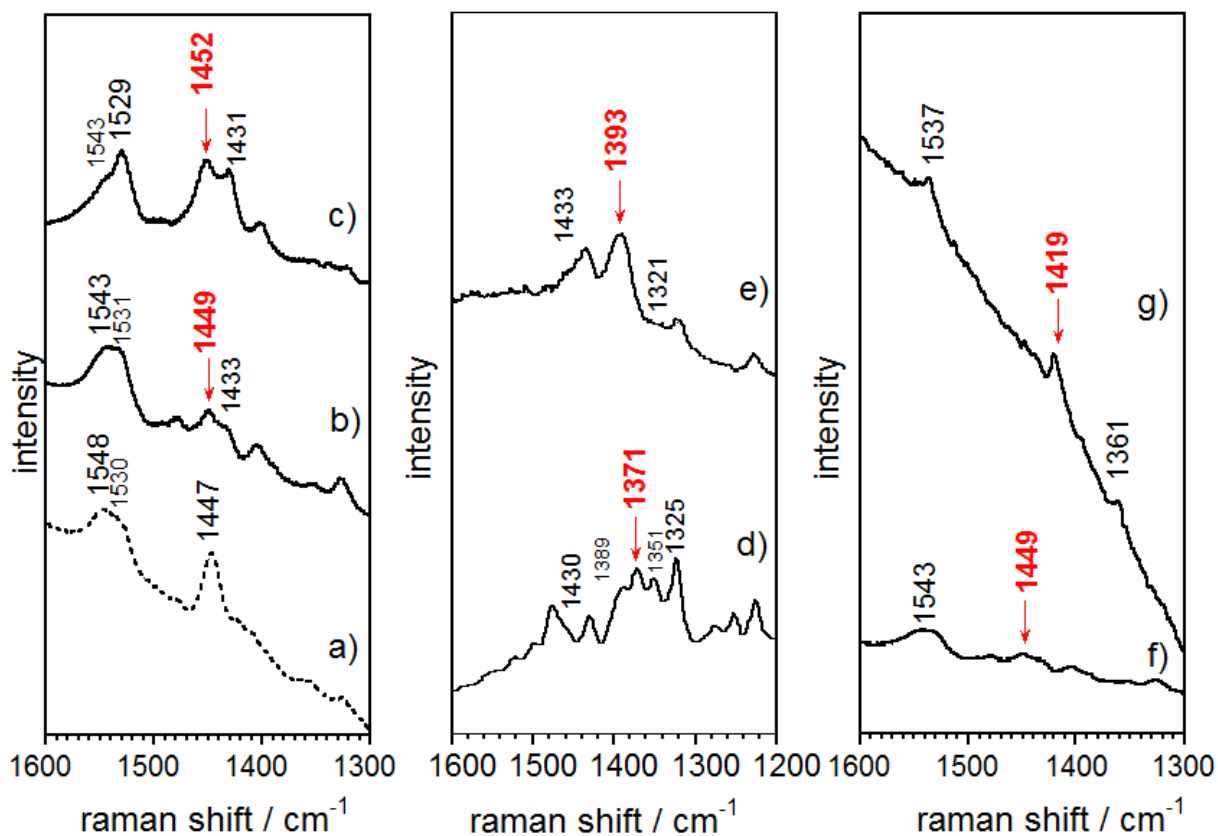

Figure 10. 532 nm Raman spectra in solid state of: a) neutral **BPY-2T**, b) neutral **BPY-2T-N(*i*-Pr)$_2$**, c) neutral **BPY-3T-N(Me)$_2$**, d) oxidized **BPY-2T-N(*i*-Pr)$_2$**, e) oxidized **BPY-3T-N(Me)$_2$**, f) neutral **BPY-2T-N(*i*-Pr)$_2$** and g) protonated **BPY-2T-N(*i*-Pr)$_2$**.

Oxidation of **BPY-2T-N(*i*-Pr)$_2$** and **BPY-3T-N(Me)$_2$** to their radical cations, **[BPY-2T-N(*i*-Pr)$_2$]$^{+•}$** and **[BPY-3T-N(Me)$_2$]$^{+•}$**, proceeds by electron extractions on the electron rich oligothiophene moieties which become quinoidized. Consequently the most important CC Raman stretching bands move down to 1373 cm^{-1} in the shorter oligomer, **[BPY-2T-N(*i*-Pr)$_2$]$^{+•}$**, and slightly higher at 1393 cm^{-1} in **[BPY-3T-N(Me)$_2$]$^{+•}$**.[25] This data is consistent with the Raman spectra of oxidized oligomers previously investigated.

Protonation of **BPY-2T-N(*i*-Pr)$_2$** (Figure 10) results in the appearance of a new band at 1419 cm^{-1} in the thienyl CC stretching region. The downshift from 1449 cm^{-1} to 1419 cm^{-1} after protonation must be explained by the larger quinoidization of the bithiophene segment due to the new role of the amino nitrogen which changes from a strong electron releasing group in neutral **BPY-2T-N(*i*-Pr)$_2$** to a electron withdrawing group in **BPY-2T-N$^+$H(*i*-Pr)$_2$**. The BODIPY CC stretching band also downshifts by 6 cm^{-1} upon protonation.[26]

IV. Conclusions.

We have synthesized new push-pull oligothiophenes based on the BODIPY group as the electron acceptor and *N,N*-dialkylamino-oligothiophenes as the donor moiety in order to enhance the electronic properties. A complete characterization of the electronic properties and molecular structures has been done consisting of the analysis of their photophysical, electrochemical and vibrational properties. In this regard, these samples can be termed as NIR dyes (i.e., note that NIR dyes are noted for absorption larger than 700 nm) and amphoteric redox electroactive molecules. We have described the presence dual fluorescence resulting from intramolecular charge transfer states (i.e., TICT states) and explain the extent of the emission on the basis of bithiophene to BODIPY energy transfer (Förster mechanism) for **BPY-2T**. As for the push-pull molecules, **BPY-2T-N(*i*-Pr)$_2$** and **BPY-3T-N(Me)$_2$**, the quenching of the fluorescence is likely due to the electron exchange by a Dexter-type mechanism. The important role of the N,N-dialkylamino groups has

been examined which provokes excitations between the BODIPY and thienyl groups with donor→acceptor and inverse acceptor→donor character which are the basis for the ICT processes in the photophysics and the appearance of stable oxidation and reductions in the electrochemistry.

Suitable reactions such as protonation and selective chemical oxidation on these derivatives have been described and valuable proton triggered and electrochromic properties have been found and interpreted. From the point of view of material applications, these systems can be used for solar cell applications due to both the good Vis-NIR absorbing characteristics and ambipolar redox behavior which is a key requirement to attain high yields of charge separated states after light absorption. More work to test these electro-optical properties is underway.

Supporting Information. Additional spectroscopic, photophysical and computational details are provided.

References.

[1]. Mishra, A.; Ma, C.-Q.; Baüerle, P. *Chem. Rev.* **2009**, *109*, 1141. Roncali, J. *Chem. Rev.* **1997**, *97*, 173. Fichou, D. *J. Mater. Chem.* **2000**, *10*, 571−588. Shirota, Y. *J. Mater. Chem.* **2000**, *10*, 1. Mitschke, U.; Baüerle, P. *J. Mater. Chem.* **2000**, *10*, 1471. *Handbook of*

Thiophene-Based Materials: Applications in Organic Electronics and Photonics, Perepichka, I. F. and Perepichka, D. F. (Eds). Wiley, **2009**. *Organic Electronics*; Klauk, H., Ed.; Wiley-VCH: Weinheim, 2006**.**

[2].   a) Garnier, F.; Hajlaoui, R.; Yassar, A.; Srivastava, P. *Science* **1994**, *265*, 1684. b) Li, X.-C.; Sirringhaus, H.; Garnier, F.; Holmes, A. B.; Moratti, S. C.; Feeder, N.; Clegg, W.; Teat, S. J.; Friend, R. H.   *J. Am. Chem. Soc.* **1998**, *120*, 2206. c) Laquindaum, J. G.; Katz, H. E.; Lovinger, A. J. *J. Am. Chem. Soc.* **1998**, *120*, 664. d) Ponomarenko, S.; Kirchmeyer, S.; Elschner, A.; Huisman, B. H.; Karbach, A.; Dreschler, D. *Adv. Funct. Mater.* **2003**, *13*, 591. e) Mushrush, M.; Facchetti, A.; Lefenfeld, M.; Katz, H. E.; Marks, T. J. *J. Am. Chem. Soc.* **2003**, *125*, 9414. f) Newman, C. R.; Frisbie, C. D.; da Silva Filho, D. A.; Brédas, J. L.; Ewbank, P. C.; Mann, Kent R.   *Chem. Mater.*, **2004**, *16*, 4436. g) Pappenfus, T. M.; Chesterfield, R. J.; Frisbie, C. D.; Mann, K.R.; Casado, J.; Raff, J. D.; Miller, L. L. *J. Am. Chem. Soc.* **2002**, *124*, 4184. h) Chesterfield, R. J.; Newman, C. R.; Pappenfus, T. M.; Ewbank, P. C.; Haukaas, M. H.; Mann, K. R.; Miller, L. L.; Frisbie, C. D. *Adv. Mater.* **2003**, *15*, 1278.   i) Dimitrakopoulos, C. D.; Malenfant, P. R. L. *Adv. Mater.* **2002**, *14*, 99. j) Otsubo, T.; Aso, Y.; Takimiya, K. *J. Mater. Chem.* **2002**, *12*, 2565.

[3].   Roncali, J. *Chem. Soc. Rev.* **2005**, *34*, 483. Lu, J.; Xia, P. F.; Lo, P. K.; Tao, Y.; Wong, M. S.   *Chem. Mater.* **2006**, *18*, 6194. Li, Zhong H.; Wong, M. S.; Tao, Ye; Fukutani, H.. *Org. Lett.*, **2007**, *9*, 3659. Perepichka, I. F.; Perepichka, D. F.; Meng, H.; Wudl, F. *Adv. Mater.* **2005**, *17*, 2281. Suzuki, M.; Fukuyama, M.; Hori, Y.; Hotta, S. *J. Appl. Phys.* **2002**, *91*, 5706. Hiramatsu, T.; Shimada, T.; Hotta, S.; Yanagi, H. *Thin Solid Films* **2008**, *516*, 2700. Barbarella, G.; Favaretto, L.; Sotgiu, G.; Zambianchi, M.; Fattori, V.; Cocchi, M.; Cacialli, F.; Gigli, G.; Cingolani, R. *Adv. Mater.* **1999**, *11*, 1375. Barbarella, G.; Favaretto, L.; Sotgiu, G.; Zambianchi, M.; Bongini, A.; Arbizzani, C.; Mastragostino, M.; Anni, M.; Gigli, G.; Cingolani, R. *J. Am. Chem. Soc.* **2000**, *122*, 11971. Barbarella, G.; Melucci, M.; Sotgiu, G. *Adv. Mater.* **2005**, *17*, 1581. Pina, J.; Seixas de Melo, J.; Burrows, H. D.; Batista, R. M. F.; Costa, S. P. G.; Raposo, M. M. M. *J. Phys. Chem. A* **2007**, *111*, 8574.

[4].   Barbarella, G.; Favaretto, L.; Sotgiu, G.; Zambianchi, M.; Fattori, V.; Cocchi, M.; Cacialli, F.; Gigli, G.; Cingolani, R. *Adv. Mater.* **1999**, *11*, 1375. Barbarella, G.; Favaretto, L.; Sotgiu, G.; Zambianchi, M.; Bongini, A.; Arbizzani, C.; Mastragostino, M.; Anni, M.; Gigli, G.; Cingolani, R. *J. Am. Chem. Soc.* **2000**, *122*, 11971. Barbarella, G.; Melucci, M.; Sotgiu, G. *Adv. Mater.* **2005**, *17*, 1581. Garnier, F., Horowitz, G.; Valat, P.; Fayçal, K.; Wintgens, V. *App. Phys.Lett.* **1998**, *72*, 2087. Samuel, I.D.W.; Turnbull, G.A. *Chem. Rev.*

2007, *107*, 1272. Yamao, T.; Yamamoto, K.; Taniguchi, Y.; Hotta, S. App.Phys. Lett. **2007**, *91*, 201117/1. Bando, K.; Nakamura, T.; Masumoto, Y.; Sasaki, F.; Kobayashi, S.; Hotta, S. *J. App. Phys.*, **2006**, *99*, 013518/1. Ichikawa, M.; Hibino, R.; Inoue, M.; Haritani, T.; Hotta, S.; Koyama, T.; Taniguchi, Y. *Adv. Mater.*, **2003**, *15*, 213.

[5]. Schueppel, R.; Schmidt, K.; Uhrich, C.; Schulze, K.; Wynands, D.; Bredas, J. L.; Brier, E.; Reinold, E.; Bu, H. B.; Baüerle, P.; Maennig, B.; Pfeiffer, M.; Leo, K. *Phys. Rev. B* **2008**, *77*, 085311. Hara, K.; Wang, Z.-S.; Sato, T.; Furube, A.; Katoh, R.; Sugihara, H.; Dan-oh, Y.; Kasada, C.; Shinpo, A.; Suga, S. *J. Phys. Chem. B* **2005**, *109*, 15476. Wang, Z.-S.; Cui, Koumura, N.; Wang, Z.-S.; Mori, S.; Miyashita, M.; Suzuki, E.; Hara, K. *J. Am. Chem. Soc.* **2006**, *128*, 14256. Wang, Z.-S.; Koumura, N.; Cui, Y.; Takahashi, M.; Sekiguchi, H.; Mori, A.; Kubo, T.; Furube, A.; Hara, K. *Chem. Mater.* **2008**, *20*, 3993. Fischer, M. K. R.; López-Duarte, I.; Wienk, M.M.M.; MartÍnez-Díaz, V.; Janssen, R. A. J.; Baüerle, P.; Torres, T. *J. Am. Chem. Soc.* **2009**, 131, 8669.

[6]. Marder, S. R.; Gorman, C. B.; Tiemann, B. G.; Cheng, L. T. *J. Am. Chem Soc.* **1993**, *115*, 3006. Marder, S. R.; Cheng, L. T.; Tiemann, B. G. *J. Chem. Soc., Chem. Commun.* **1992**, 672. Marder, S. R.; Cheng, L. T.; Tiemann, B. G.; Friedli, A. C.; Blanchard-Desce, M.; Perry, J. W.; Skindhoj, J. *Science* **1994**, *263*, 511. Costa, S. P. G.; Batista, R. M. F.; Cardoso, P.; Belsey, M.; Raposo, M. M. M. *Eur. J. Org. Chem.* **2006**, *17*, 3938. Batista, R. M. F.; Costa, S. P. G.; Lodeiro, C.; Belsley, M.; Raposo, M. M. M. *Tetrahedron* **2008**, *64*, 9230. Raposo, M. M. M.; Ferreira, A. M. F. P.; Belsley, M.; Moura, J. C. V. P. *Tetrahedron* **2008**, *64*, 5878. Herbivo, C.; Comel, A.; Kirsch, G.; Fonseca, A. M. C.; Belsley, M.; Raposo, M. M. M. *Dyes Pigments* **2010**, *82*, 217.

[7]. Barbarella, G.; Melucci, M.; Sotgiu, G. *Adv. Mater.* **2005**, *17*, 1581. Ridolfi, G.; Camaioni, N.; Samori, P.; Gazzano, M.; Accorsi, G.; Armaroli, N.; Favaretto, L.; Barbarella, G. *J. Mater. Chem.* **2005**, *15*, 895. Mariano, F.; Mazzeo, M.; Duan, Y.; Barbarella, G.; Favaretto, L.; Carallo, S.; Cingolani, R.; Gigli, G. *App. Phys. Lett.* **2009**, *94*, 063510.

[8] Loudet, A.; Burgess, K. *Chem. Rev.* **2007**, 4891; Gilles Ulrich, Raymond Ziessel, Anthony Harriman, *Angew. Chem. Int. Ed.* **2008**, *47*, 1184.

[9]. A. C.; Benniston, A. C.; Copley, G.; Harriman, A.; Rewinska, D. B. *J. Am. Chem. Soc.* **2008**, *130*, 7174. Zrig, S.; Rémy, P.; Andrioletti, B.; Rose, E.; Asselberghs I.; Clays, K. *J. Org. Chem.* **2008**, *73*, 1563

[10]. Effenberger, F.; Schlosser, H.; Bauerle, P.; Maier, S.; Port,H.; Wolf, H. C. *Angew. Chem., Int. Ed. Engl.* **1988**, *27*, 281-284. Holl, N.; Port, H.; Wolf, H. C.; Strobel, H.;

Effenberger, F. *Chem. Phys.* **1993**,*176,215.* Casado, J.; Hernández, V.; Ruiz Delgado, M. C.; López Navarrete, J. T.; Pappenfus, T. M.; Williams, N.; Stegner, W. J.; Johnson, J. C.; Edlund, B. A.; Janzen, D. E.; Mann, K. R.; Orduna, J.; Villacampa. B. *Chem. Eur. J.***2006**, *12*, 5458. Moreno Oliva, M.; Casado, J.; Raposo, M.M.M.; Fonseca, A.M.C.; Hartmann, H.; Hernández, V.; López Navarrete, J.T. *J. Org. Chem.* **2006**, *71*, 7509. Casado, J.; Pappenfus, T. M.; Miller, L. L.; Mann, K. R.; Ortí, E.; Viruela, P. M.; Pou-Amérigo, R.; Hernández, V.; López Navarrete, J. T. *J. Am. Chem Soc.***2003**, *125*, 2524.

[11]. Raposo, M. M. M.; Kirsch, G. Tetrahedron, 2003, 59(26), 4891-4899; Raposo, M. M. M.; Fonseca, A. M. C.; Kirsch, G. Raposo, *Tetrahedron* **2004**, *60*, 407.

[12]. Eaton, D. F. *Pure Appl. Chem.* **1988**, *84*, 1871.

[13]. P.J. Stephens, F.J. Devlin, F.C.F. Chabalowski, M.J. Frisch, *J. Phys. Chem.* **1994**, *98*, 11623; J.J. Novoa, C. Sosa, *J. Phys. Chem.* **1995**, *99*, 15837; E. Casida, C. Jamorski, K.C. Casida, D.R. Salahub, *J. Chem. Phys.* **1998,** *108*, 4439; R.E. Stratman, G.E. Scuseria, M.J. Frisch, *J. Chem. Phys.* **1998,** *109*, 8218.

[14]. Gross, E. K. U.; C. A. Ullrich and U. J. Gossman (1995). E. K. U. Gross and R. M. Dreizler. ed. *Density Functional Theory*. B. **337**. New York: Plenum Press. Runge, E.; Gross, E.K.U. *Phys. Rev. Lett.,* **1984**, *52*, 997.

[15]. J.B. Foresman, M. Head-Gordon, J.A. Pople, M.J. Frish, *J. Phys. Chem.* **1992**, *96*, 135.

[16]. Gaussian 03, Revision C.02, Frisch, M. J.; Trucks, G. W.; Schlegel, H. B.; Scuseria, G. E.; Robb, M. A.; Cheeseman, J. R.; Montgomery, Jr., J. A.; Vreven, T.; Kudin, K. N.; Burant, J. C.; Millam, J. M.; Iyengar, S. S.; Tomasi, J.; Barone, V.; Mennucci, B.; Cossi, M.; Scalmani, G.; Rega, N.; Petersson, G. A.; Nakatsuji, H.; Hada, M.; Ehara, M.; Toyota, K.; Fukuda, R.; Hasegawa, J.; Ishida, M.; Nakajima, T.; Honda, Y.; Kitao, O.; Nakai, H.; Klene, M.; Li, X.; Knox, J. E.; Hratchian, H. P.; Cross, J. B.; Bakken, V.; Adamo, C.; Jaramillo, J.; Gomperts, R.; Stratmann, R. E.; Yazyev, O.; Austin, A. J.; Cammi, R.; Pomelli, C.; Ochterski, J. W.; Ayala, P. Y.; Morokuma, K.; Voth, G. A.; Salvador, P.; Dannenberg, J. J.; Zakrzewski, V. G.; Dapprich, S.; Daniels, A. D.; Strain, M. C.; Farkas, O.; Malick, D. K.; Rabuck, A. D.; Raghavachari, K.; Foresman, J. B.; Ortiz, J. V.; Cui, Q.; Baboul, A. G.; Clifford, S.; Cioslowski, J.; Stefanov, B. B.; Liu, G.; Liashenko, A.; Piskorz, P.; Komaromi, I.; Martin, R. L.; Fox, D. J.; Keith, T.; Al-Laham, M. A.; Peng, C. Y.; Nanayakkara, A.; Challacombe, M.; Gill, P. M. W.; Johnson, B.; Chen, W.; Wong, M. W.; Gonzalez, C.; and Pople, J. A.; Gaussian, Inc., Wallingford CT, 2004.

[17]. Becke, A. D. *J. Chem. Phys.* **1993**, *98*, 1372.

[18]. Francl, M. M.; Pietro, W. J.; Hehre, W. J.; Binkley, J. S.; Gordon, M. S.; Defrees, D. J.; Pople, J. A. *J. Chem. Phys.* **1982**, *77*, 3654.

[19]. Deniz, Yilmaz M.; Altan Bozdemir, O.; U. Akkaya, E, *Org. Lett.* **2006**, *8*, 2871.

[20]. Effenberger, F.; Würthner, F.; and Steybelb, F. *J. Org. Chem.* **1995**, *60*, 2082.

[21]. Koopmans, T. *Physica* **1934**, *1*, 113.

[22]. Kim, Y.H.; Cho, D.W.; Yoon M. ; Kim. D. *J. Phys. Chem.* **1996**, *100*, 15670.

[23]. Modern Molecular Photochemistry; N. J. Turro, 1991.

[24]. Hernández, V.; Casado, J.; Effenberger, F.; López Navarrete, J. T. *J. Chem. Phys.* **2000**, *112*, 5105.

[25]. J. Casado, V. Hernández, S. Hotta, J.T. López Navarrete, *J. Chem. Phys.* **1998**, *109*, 10419; J. Casado, V. Hernández, S. Hotta, J.T. López Navarrete, *Adv. Mater.* **1998**, *10*, 1258; J. Casado, L.L. Miller, K.R. Mann, T.M. Pappenfus, Y. Kanemitsu, E. Orti, P.M. Viruela, P. Pou-Amerigo, V. Hernández, J.T. López Navarrete, *J. Phys. Chem. B* **2002**, *106*, 3872; J. Casado, L.L. Miller, K.R. Mann, T.M. Pappenfus, V. Hernández, J.T. López Navarrete, *J. Phys. Chem. B* **2002**, *106*, 3597.

[26]. Hernández, V.; Muguruma, H.; Hotta, S.; Casado, J.; López Navarrete, J. T. *J. Phys. Chem. A*, **2000**, *104*, 735.